Kinetics of Aggregation of Denatured Proteins I

Methodology Based on the Multichannel Particle Size Analyzer

By NORMAN F. H. HO and WILLIAM I. HIGUCHI

The purpose of this study was to develop a method for studying the kinetics and the mechanisms of aggregation of denatured protein particles. It was found that a procedure based on the RIDL multichannel particle counter and size analyzer system was suitable. The precipitation behavior of urea denatured ovalbumin was studied near its isoelectric point. An evaluation of the data showed that the Smoluchowski theory for rapid aggregation of monodispersed particles and the self-preservation theory satisfactorily accounted for the results.

THE PROPENSITY of proteins to undergo gross physical and chemical changes by denaturation is realized in clinical biochemistry. This characteristic property is the basis for diagnostic procedures involving sedimentation, salt precipitation, and heat coagulation of proteins, such as the erythrocyte sedimentation reaction, the Weltman coagulation band technique, turbidity, and flocculation reactions (1, 2). More recently, medical researchers have developed the use of denatured protein particles complexed with radioisotopes to measure renal, liver, splenic, and pulmonary blood flow (3–5). One preparation, *i.e.*, the particle denatured human serum albumin —^{131}I complex, is used for the rapid diagnosis and location of pulmonary embolism by scintillation scanning on the basis of differential filtration of the tracer particles at the site of embolism (6). The particle size and stability of the suspension are critical problems of this preparation.

While the protein chemists have intensified their investigations on the denatured protein mainly in the direction to unravel the structure of the native protein and to study the kinetics, mechanisms, and energetics of the denaturation process itself, the kinetics of growth and aggregation of denatured protein particles has received little or no attention. Research on the particulate behavior of denatured proteins should contribute to the fundamental understanding of the techniques in clinical laboratory procedures involving sedimentation of denatured proteins and in the interpretation of relevant data. In the field of applied pharmaceutical chemistry, such studies should provide a basic approach to the preparation of protein particles tagged with radioactive substances for the rapid diagnosis of embolism. Through the application of controlled growth and aggregation, one should be able to "tailor-make" a stable denatured protein particle or aggregate of uniform and desired size.

The long range objective of the present research is to study this aspect of denaturation on a quantitative basis. The authors hope to examine the effects of protein species and concentration, the method of denaturation, pH, temperature, mono- and polyvalent electrolytes, solvents, and surface-active agents.

The purpose of this paper is to present a well-defined procedure for carrying out such studies. It involves the use of an electronic resistance counter with a multichannel particle size analyzer to follow changes in particle size distributions with time. For the model system studied here, the urea–pH induced denaturation of ovalbumin (7) was chosen taking advantage of the well-defined properties and the better controlled irreversible denaturation of ovalbumin.

EXPERIMENTAL

Materials and Method of Denaturation.—A single lot of twice crystallized, lyophilized ovalbumin[1] was used throughout the study without further recrystallization and stored in a tight container under refrigeration to maintain stability of the protein. Urea used was reagent grade. Buffer solutions were prepared from reagent grade salts and standardized with the Beckman zeromatic pH meter.

One-half and 1% ovalbumin solutions in 8 *M* urea–phosphate buffer were prepared in the following manner. Ovalbumin was dissolved in a small amount of 0.05 *M* phosphate buffer (pH 6.88 and previously filtered through 0.45 μ Millipore filters) without stirring. To this was added the freshly prepared phosphate buffered urea solution with gentle stirring. The final pH was 7.1. Denaturation of the protein was carried out at constant stirring of 20 r.p.m. with a synchronous motor and in a closed system thermostated at 30°. At the end of 5 days, the denatured protein solution was discarded to avoid the complications of cyanate formation from the alkaline hydrolysis of urea (8).

Procedure for Aggregation[2] Studies.—Samples of the urea-denatured ovalbumin were used for the

Received April 28, 1966, from the College of Pharmacy, University of Michigan, Ann Arbor.

Accepted for publication October 13, 1966.

Presented to the Basic Pharmaceutics Section, A.PH.A. Academy of Pharmaceutical Sciences, Dallas meeting, April 1966.

This investigation was supported by fellowship 5-F1-GM-24,039 from the Institute of General Medical Sciences, National Institutes of Health, U. S. Public Health Service, Bethesda, Md.

[1] Worthington Biochemical Corp., Freehold, N. J.

[2] Throughout this study "aggregation" means the formation of conglomerates of particles as distinguished from molecular aggregation.

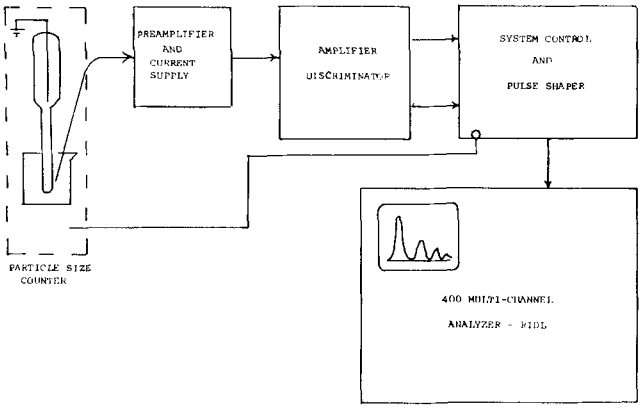

Fig. 1.—Particle counter and size analyzer system.

aggregation experiments after the viscosities of the solutions became constant. The viscosities were followed with an Ostwald viscometer. After denaturation periods of at least 18 hr., the protein solutions were diluted into 0.01 *M* acetate–normal saline buffer solutions, previously adjusted to pH 4.6 or 5.5, so that the final concentration was 1 mcg. denatured protein per ml. Also, normal saline adjusted to pH 8.7 with sodium hydroxide was used as a diluting solution. Initially, the solutions were mixed with gentle stirring and then allowed to stand without disturbance. Dilutions were made for several denaturation periods. The course of the aggregation with time was followed by the single channel Coulter counter, model A, and the RIDL multichannel particle analyzer. Both the 30-μ and 50-μ aperture tubes were used. For the counting runs, a further 1:11 dilution of the master suspension was necessary to minimize coincidence errors. The initial particle concentrations were in the neighborhood of 1×10^7 particles per ml. Since the aggregating system was somewhat sensitive to the method of dilution, a procedure was developed that did not influence the results. A 1-ml. transfer pipet, Kimax -51 No. 37034-A, blow-out type, was used to pipet and deliver an aliquot at the rate of 1 ml./15 sec. The delivery was performed with the tip of the pipet under the surface of the diluting medium and the remaining drops were gently blown out. The samples were then immediately counted.

Particle Counter and Size Analyzer System and Its Standardization.—To follow aggregation, changes in the particle size distribution as a function of time were followed by a new electronic resistance counter system shown schematically in Fig. 1. The system consists of a particle detector apparatus based on the Coulter counter[3] principle and a sophisticated transistorized RIDL 400 channel analyzer,[4] which was originally developed for γ-ray spectrometry. A constant current is supplied to the aperture tube of the detector apparatus. As a particle moves through the aperture, there is an abrupt change in the aperture current. The current signal is amplified and converted to a voltage pulse by the preamplifier. The pulse is then shaped and sent on to the pulse height analyzer where it is classified into one of the 400 channels and counted. Only one pulse can be analyzed at a time, but the analyzer performs this task in the order of milliseconds before accepting another pulse.

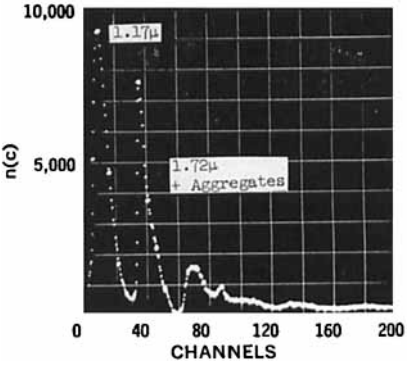

Fig. 2.—Differential distribution data for a mixture of a 1.17 and 1.72-μ diameter latices. Two-hundred channels used. n(c) is the concentration of particles in channel c.

The distribution of particle size densities can be oscillographically displayed or stored in memory. By utilizing only 100 channels at a time, it is possible to simultaneously hold in memory up to four particle size distributions which may be displayed independently or simultaneously on the oscilloscope screen. Corrections for background may also be programmed.

While in most of the present work the data were presented on the oscilloscope screen and photographed with a Polaroid camera, other convenient modes of data retrieval may be used. Numerical readout devices and conventional recorders are easily adapted to the instrument.

Standardization of the multichannel particle analyzer was accomplished with 1.17, 1.72, and 2.051-μ diameter polyvinyltoluene latices[5] suspended in 0.90% sodium chloride solutions. All of the standard latices were washed repeatedly with alcohol and water by centrifugation, and the latter two latices were aggregated to some degree with magnesium sulfate. Microscopic measurements and the Coulter counter, model A, served as a check. Figure 2 shows the differential distribution of a mixture of 1.17-μ and aggregated 1.72-μ diameter

[3] Coulter Electronics, Chicago, Ill.
[4] Radiation Instrument Development Laboratory, Inc., Melrose, Park, Ill.
[5] Dow Chemical Co., Midland, Mich.

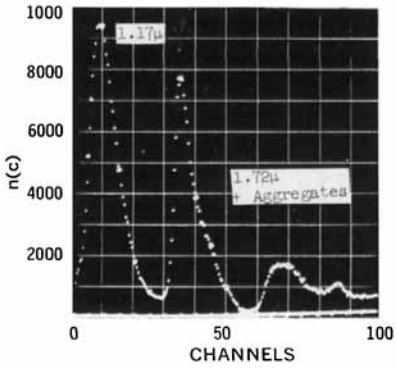

Fig. 3.—Same distribution as Fig. 2, but only the first 100 channels presented.

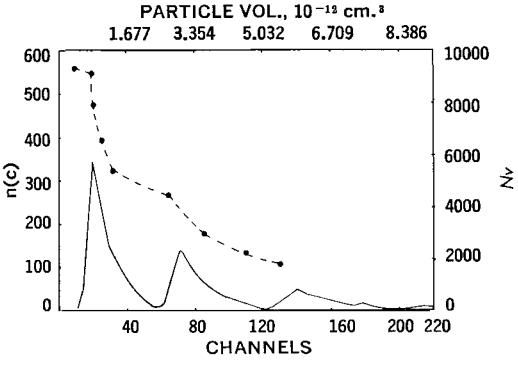

Fig. 4.—Analysis of a mixture of the 1.17-μ and an aggregated 1.72-μ diameter latices. Key: ———, differential distribution data obtained with multichannel system; – – – –, data obtained with Coulter counter, model A.

latices. It is the oscillographic spectrum actually displayed by the 400 multichannel analyzer. Here, however, only 200 channels have been used to describe the distribution. The channel number is proportional to particle volume and the x-axis is calibrated with at least two known standards. The total number of particles corresponding to a given channel is represented by a point so that there will be as many points on the smooth distribution curve as there are preselected number of channels. At the 10th channel in Fig. 2, there is essentially a unimodal distribution of the 1.17-μ particles. The sharp singlet peak for the 1.72-μ particles occurs at about the 35th channel, its doublet peak occurs at approximately the 70th channel, and the triplet aggregate at the 105th channel as expected. However, there is in addition an odd small peak at the 90th channel.[6] The somewhat broader distributions of the high order aggregates are probably due to the wider distributions of shapes (configurations).

[6] Tentatively, the authors have assigned both peaks at the 90th and 105th channels to triplet aggregates. Microscopically, the triplet aggregates appear in three general geometrical forms, *viz.*, the triangular, linear, and other angular arrangements. According to rough theoretical calculations on the effect of particle shape factors on the electronic particle detection system and qualitative experimental data on the rearrangement kinetics of the triplet aggregates, there would be approximately a spread of 10 to 20 channels between the more stable triangular triplet aggregate and the other triplet aggregates. This study is being pursued further.

The distribution of the 1.72-μ latices shows about 45% aggregation. When longer sampling times were taken, the statistics for the higher order aggregates improved and even 8-mers were detectable for the 1.72-μ aggregated system at approximately the 285th channel. There is relatively good linearity with this system. Figure 3 shows the same distribution as in Fig. 2 except that the first 100 channels have been expanded by means of the x-axis expansion control. Likewise, the second 100 channels may be expanded for examination of the higher order aggregates.

A quantitative analysis of a mixture of 1.17 and aggregated 1.72-μ latices was carried out with both the multichannel particle analyzer and the Coulter counter, model A, using a 30-μ aperture tube. As shown in Fig. 4, the multichannel analyzer gives directly a differential distribution, while the Coulter counter gives a cumulative distribution. Whereas the differential distribution data were obtained from one 50-μl. sample, the cumulative distribution was obtained with nine 50-μl. samples. The advantages of the multichannel system can be seen from Fig. 4. With the single channel instrument many sample readings must be taken to achieve the same degree of accuracy. For example, if the sixth point in the cumulative plot of Fig. 4 were not taken, it would have been impossible to decide whether the first two peaks were separate or possibly a single broad distribution. Also, the true particle distribution cannot be adequately resolved for rapid flocculating systems without laborious effort.

To compare the data from the multichannel analyzer with that from the Coulter counter, the differential distributions were integrated planimetrically. Therefore,

$$N_v = \int_v^\infty n(v)dv \qquad \text{(Eq. 1)}$$

where N_v is the integral number of particles larger than v, and $n(v)dv$ is the number of particles between the sizes v and $v + dv$. The results are tabulated (Table I) and compared with the Coulter counter data.

As the sophistication of the electronics of the multichannel analyzer allows one to detect rapid changes in particle size distributions, the direct display of the differential distribution and the efficient data recording techniques can be utilized with the aid of Eq. 1 to follow the course of aggregation of an initially monosized particle system as a function of time.

Recently, Samyn (9) reported that when suspension systems are highly polydispersed, the Coulter

Table I.—Comparison of Coulter Counter, Model A, and RIDL Multichannel Data on Mixed Latex Particles

Channels	Particle Vol. 10^{-12} cm.³	No. of Particles Beyond Stated Size: RIDL Multichannel	No. of Particles Beyond Stated Size: Coulter, Model A
10	0.419	9256	9350
20	0.839	8462	8550
40	1.677	5421	5350
60	2.51	4760	4700
80	3.354	3239	3300
100	4.193	2380	2400
120	5.032	1851	1850

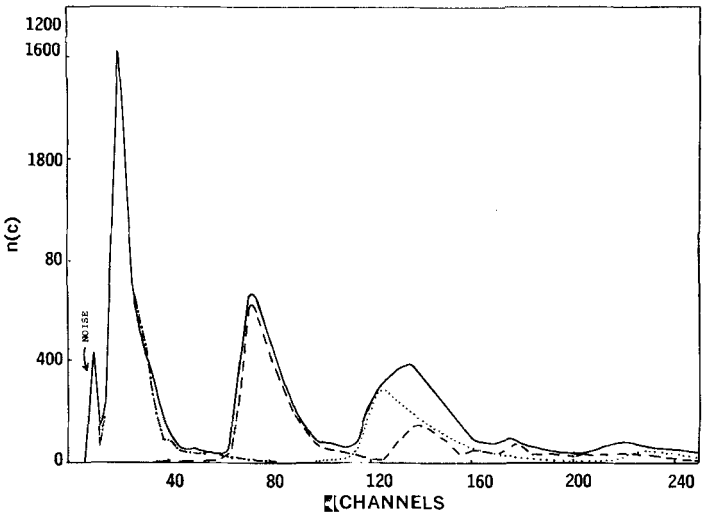

Fig. 5.—Distribution curves accounting for additivity in a polydispersed latex system by the RIDL multichannel analyzer. Key: ———, distributions of mixture of equal parts of 1.17, 1.72, and 2.05 μ; —·—·—, independent distribution of 1.17 μ; — — —, independent distribution of 1.72 μ; ....., independent distribution of 2.05 μ.

counter, model A, may show poor additive results. This prompted the investigation of the reliability of the multichannel analyzer in this aspect, at least in the range of sizes pertinent to our research. Figure 5 shows (broken curves) the independent distributions of 1.17-μ and aggregated 1.72 and 2.05-μ particles. The noise peak at the 10th channel serves as a reference from which the true particle distribution can be differentiated. Upon mixing equal parts of the latex suspensions, the resulting normalized distribution assuming additivity of the separate runs is shown by the smooth curve. It appears therefore that the multichannel analyzer system can give accurate results even when the polydispersity is of the order of thirtyfold in volume.

Because the latex particles are essentially monodisperse, the peak widths given in Figs. 2–5 may be used to estimate the instrument resolution. In the present size range this is found to be about ± 0.1 to 0.2 μ in the diameter. Except in unusual situations, most real suspension systems have broad enough particle size distributions so that the instrument resolution does not constitute a serious limitation.[7]

RESULTS AND DISCUSSION

Process of Denaturation.—The kinetics and mechanisms of denaturation of ovalbumin by urea are discussed in a number of references (7, 10–13). The initial stage is an intramolecular reaction involving the destruction of internal order. This may be interpreted as the unfolding of the helical structures of ovalbumin to a more randomly coiled arrangement accompanied by an increase in viscosity. Usually, this stage is measured by optical rotation. The second stage is characterized by an increase in viscosity of the solution without further change in optical rotation. In contrast to the relatively rapid increase in viscosity in the initial stage, the viscosity increases at a slower rate during this second stage and eventually reaches a plateau. It is believed that association of the denatured protein molecules primarily by exchange reaction with sulfhydryl and disulfide groups is an important factor in this second phase. In general, the concentrations of ovalbumin, urea and electrolytes, pH, and temperature all affect this over-all denaturation process.

With the ovalbumin–urea concentration ratios used in this study, the first stage of denaturation is completed within 3 hr. and the viscosity reached a plateau a few hours thereafter.

Aggregation Experiments.—Typical differential particle distributions at various time intervals, obtained directly from photographs of the oscillographic display of the multichannel analyzer, are shown in Fig. 6 for the aggregation of denatured protein. In this instance the 30-μ aperture tube was used. Since there was a noise contribution in channels 10 to 13, previously pointed out in Fig. 5, only that portion of the distribution from the 15th channel was used for further analysis.

Figure 7 gives the cumulative counts *versus* time curves showing aggregation of denatured ovalbumin at times greater than about 60 min. These results were planimetrically determined from data such as those given in Fig. 6. The pH is in the neighborhood of the isoelectric point for denatured ovalbumin. The two curves correspond to the 0.5% and the 1.0% protein denatured for 24 and 22 hr., respectively. For longer denaturation times the results were essentially the same.

Mass balance was approximately maintained after times greater than the time corresponding to the peak shown in Fig. 7. This was established by graphical integration,

$$M = \int_v^\infty \rho v n(v) dv \qquad \text{(Eq. 2)}$$

where M is the protein mass, ρ is the density, v is the volume of the particle, and $n(v)dv$ is the number of particles between the sizes v and $v + dv$.

The range of sizes observed in these experiments was 0.4 to 1.2-μ radius. The majority of the particles were between 0.4 to 0.8-μ radius. Under the microscope, $\times 970$ in immersion oil, aggregates were found to be nearly spherical in shape and were in the general magnitude of sizes detected by the multichannel analyzer.

[7] A detailed study of this question is underway and will be reported in a later communication.

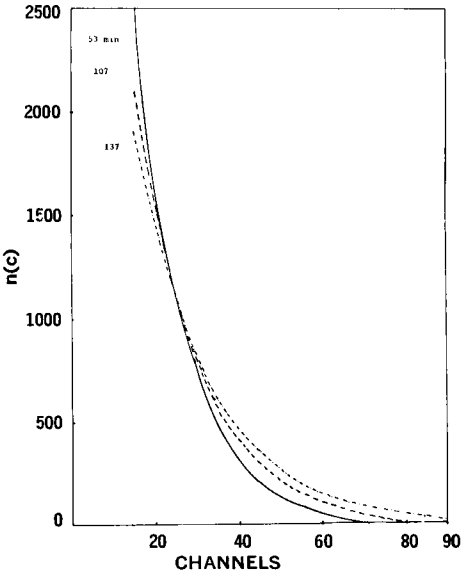

Fig. 6.—Differential distribution data showing aggregation of denatured ovalbumin particles with time in buffered saline, pH = 4.6.

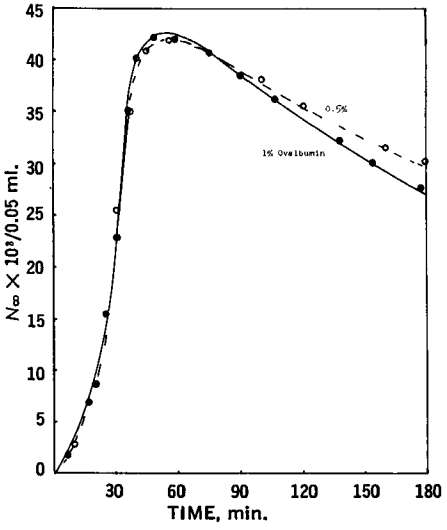

Fig. 7.—Changes in total denatured protein particulate concentration for sizes greater than 0.80-μ diameter as a function of time. Decreasing counts after 60 min. reflect aggregation of particles.

Comparison with Smoluchowski's Theory.—Smoluchowski worked out a basic theory of aggregation of spherical particles of a colloidal suspension (14). When the aggregation is controlled by Brownian diffusion in the absence of a force field, the aggregation of a relatively monodispersed system is given by the kinetic expression for bimolecular collision,

$$\frac{dN_\infty}{dt} = -KN_\infty^2 \qquad \text{(Eq. 3)}$$

Where N_∞ is the number of particles of all sizes, K is the rate constant, and t the time. Upon integration a linear relationship of $1/N_\infty$ *versus* t with slope K is predicted. For this case, the rate constant is:

$$K = \frac{4\pi DR}{W} \qquad \text{(Eq. 4)}$$

where D is the effective diffusion coefficient, R is the distance between centers of the particles, and W is the stability factor. By assuming the Stokes-Einstein relationship for translational diffusion, *i.e.*,

$$D = \frac{kT}{6\pi\mu a} \qquad \text{(Eq. 5)}$$

and the effective collision radius, $R = 2a$, and irreversible collision, $W = 1$, where k is the Boltzmann constant, μ the viscosity of the medium, T the absolute temperature, and a the particle radius, the theoretical maximum rate constant becomes

$$K = \frac{4kT}{3\mu} \qquad \text{(Eq. 6)}$$

At 30° the value of K is 5.6×10^{-12} cm.^{3} sec.$^{-1}$.

By using Eq. 1 the changes of the cumulative number of particles, N_∞, with time were determined by graphical integration with a planimeter of such differential particle distribution data as shown in Fig. 6. In the present experiments N_∞ corresponds to the total number of particles larger than the particle volume of 0.6289×10^{-12} cm.^{3} (15th channel), although the distribution extended to smaller sizes. The Coulter counter, model A, gave this quantity directly by using the appropriate threshold setting. In Fig. 8, the straight line relationship of the Smoluchowski-type plot is found. This is consistent with the theory of aggregation of essentially monodispersed sols. The experimental rate constants obtained with the 30 and 50-μ aperture tubes were not significantly different. The data much beyond 200 min. were believed to be unreliable because of the effects of sedimentation upon the aggregation rate. According to Müller (14), at room temperature, sedimentation may significantly affect the rate constant when the radius of some of the denatured ovalbumin particles are larger than 2 to 3 μ.

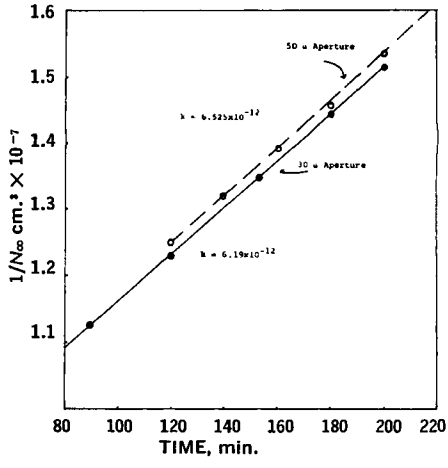

Fig. 8.—Linear plots showing agreement of the aggregation-time data with Smoluchowski theory.

In Table II the summary of some aggregation experiments of urea-denatured ovalbumin is given. The rate constant obtained from the multichannel analyzer and the Coulter counter compared well with each other and also with theory. Once the denatured protein solution reached a constant viscosity level, subsequent rate constants found did not differ from each other. There is a strong dependence of pH on the aggregation. Maximum aggregation was found near the isoelectric point. At pH 5.5 insignificant counts were detected with the 30-μ aperture tube. However, the Tyndall beam showed the presence of many submicron particles in a sol that remained stable for at least 4 weeks. At higher pH values, the Tyndall beam was weaker.

TABLE II.—SUMMARY OF DATA ON AGGREGATION OF UREA-DENATURED OVALBUMIN

Protein Concn., %	pH Buffered Normal Saline	Denaturation Period, hr.	$k \times 10^{-12}$ (cm.^{3}sec.$^{-1}$) Coulter, Model A	RIDL Multichannel
0.5	4.6	24	5.62	6.43
		64	5.90	6.19
	5.5	64	Insignificant counts,	
	8.7	64	but weak Tyndall beam observed.	
1.0	4.6	22	...	7.23
		49	7.1	7.67
	5.5	49	Insignificant counts,	
	8.7	49	but weak Tyndall beam observed.	

Comparison with the Self-Preserving Theory.—Friedlander and Swift (15) showed that certain forms of similarity or self-preserving functions can be applied to the solution of Smoluchowski's fundamental equation for aggregation. The relations depend upon the assumptions that the particle distribution in various sizes is continuous and that a particular form of the size spectrum is invariant with time. Hidy *et al.* (16, 17) have applied the theory to the case of discontinuous particle distributions.

In the theory of Friedlander and Swift the particle distribution is expressed as:

$$n(v, t) = \frac{N_\infty^2}{\phi} \psi_1(\eta) \qquad \text{(Eq. 7)}$$

where $\psi_1(\eta)$ is a dimensionless distribution function, the constant ϕ is the total volume fraction of particles:

$$\phi = \int_0^\infty vn(v)dv \qquad \text{(Eq. 8)}$$

and η is the dimensionless volume distribution:

$$\eta = \frac{vN_\infty}{\phi} \qquad \text{(Eq. 9)}$$

When $\eta = 1$, the average size of the particles with respect to volume is predicted. Furthermore,

$$N_v = N_\infty \int_\eta^\infty \psi_1(\eta)d\eta = N_\infty \psi_2(\eta) \qquad \text{(Eq. 10)}$$

where $\psi_2(\eta)$ is the dimensionless cumulative particle distribution. The terms $n(v)$, N_v, and N_∞, as defined before, are time-dependent; ψ_1 and ψ_2 are time-independent functions and, therefore, do not depend upon the initial size distributions.

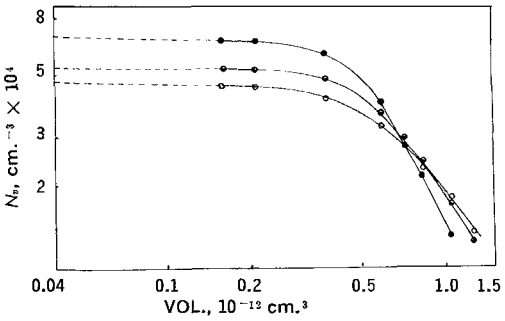

Fig. 9.—Cumulative size distributions for aggregating denatured ovalbumin particles. Key: ●, 53 min.; ◒, 107 min.; ○, 137 min.

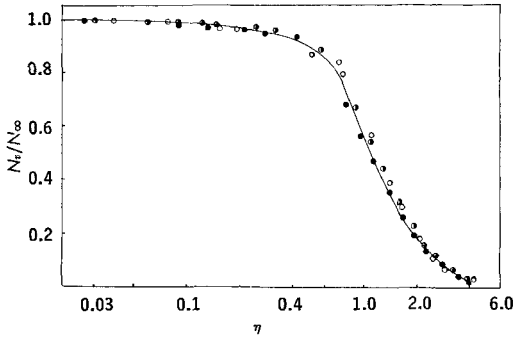

Fig. 10.—Test of self-preservation for aggregating denatured ovalbumin particles. In terms of dimensionless distribution functions, particle distributions taken at different times during the aggregation process fall approximately on a single curve. Data taken from Fig. 9.

The theory was applied to the denatured protein system for the data partially shown in Fig. 6. A log-log plot of N_v *versus* v is shown in Fig. 9 and values of N_∞ were determined by extrapolation of the curve to small values of v. When a Smoluchowski-type plot was made using the extrapolated values, the rate constant was 5.91×10^{-12} cm.^{3} sec.$^{-1}$, which is in good agreement with 6.19×10^{-12} cm.^{3} sec.$^{-1}$ previously found by using that part of the data at larger sizes. The volume fraction was 3.56×10^{-8} cm.^{3} for 0.05-ml. sample of the sol in contrast to the theoretical 3.58×10^{-8} cm.^{3} to indicate that after 53 min. practically all of the insoluble protein came into the detectable range of the RIDL analyzer system. In Fig. 10 the plots of N_v/N_∞ *versus* η at different time intervals shows the tendency of the distribution to preserve its form and gives ψ_2, the time-independent dimensionless cumulative distribution function, as predicted by Eq. 10.

According to Friedlander, if the $1/N_\infty$ *versus* t plot is linear, the rate of aggregation with the self-preserving size distribution can be described by:

$$\frac{dN_\infty}{dt} = \frac{-\alpha A_1 k T N_\infty^2}{3\mu} \qquad \text{(Eq. 11)}$$

where α is the collision efficiency having the same physical meaning as the factor W in Eq. 4, and

$$A_1 = \left[2 + 2 \int_0^\infty \eta^{1/3} d\psi_2 \int_0^\infty \eta^{-1/3} d\psi_2 \right] \quad \text{(Eq. 12)}$$

when $\alpha = 1$ and $A_1 = 4.0$, the rate constant of Eq. 11 reduces to that of Eq. 6 for the homogeneous case. Thus, A_1 is a significant parameter accounting for the effect of heterogeneity on the rate of aggregation. By comparing Eqs. 3 and 11,

$$\alpha = \frac{3K\mu}{A_1 kT} \quad \text{(Eq. 13)}$$

For the protein system, α was approximately 1, and A_1 was 4.148 ± 0.022. Then heterogeneity accounted for about 4% increase in the rate. From Eq. 11 the rate constant found was 5.81×10^{-12} cm.^{3} sec.$^{-1}$. The comparison of methods of determining the rate constant is summarized in Table III.

TABLE III.—COMPARISON OF METHODS OF DETERMINING RATE CONSTANTS OF AGGREGATION

Method of Treatment	Rate Constant, cm.^{3} sec.$^{-1}$
Smoluchowski's theory for monodispersed distribution taking N_∞ from	
(*a*) $\geq v = 0.6289 \times 10^{-12}$ cm.^{3}	6.19×10^{-12}
(*b*) $\geq v = 0.02 \times 10^{-12}$ cm.^{3}	5.91×10^{-12}
Self-preservation theory	5.81×10^{-12}

It should be noted that the approach of self-preservation theory offers a method of determining the aggregation rate constant independent of that approach which assumed a monodispersed system at initial periods of the aggregation process. Since the effective collision between particles was unity and the particle size distribution was essentially monodispersed, the rate constants determined by both methods were in good agreement.

Studies are continuing on the mechanism of the pH influence on the aggregation behavior. Experiments on the effects of electrolytes, temperature, and other additives are also planned.

REFERENCES

(1) Frankel, W., and Reitman, R., "Gradwohl's Clinical Laboratory Methods and Diagnosis," 6th ed., C. V. Mosby, St. Louis, Mo., 1964.
(2) Wuhrman, S., and Wunderly, R., "The Human Blood Proteins," Grune and Stratton, Inc., New York, N. Y., 1960.
(3) Biozzi, G., *et al.*, *J. Lab. Clin. Med.*, **51**, 230(1958).
(4) Torrance, H., and Glowenlock, A., *Clin. Sci.*, **22**, 413(1962).
(5) Taplin, G., Groswold, M., and Dore, E., *UCLA Report 481 (Biology and Medicine)*, 1961.
(6) Henkin, R., and Bishop, H., *J. Lab. Clin. Med.*, **60**, 709(1962).
(7) Simpson, R. B., and Kauzmann, W., *J. Am. Chem. Soc.*, **75**, 5139(1953).
(8) Stark, G., Stein, W., and Moore, S., *J. Biol. Chem.*, **235**, 3177(1960).
(9) Samyn, J., *J. Pharm. Sci.*, **54**, 1794(1965).
(10) Frensdorff, H., Watson, M., and Kauzmann, W., *J. Am. Chem. Soc.*, **75**, 5157(1953).
(11) Steven, F., and Tristam, G., *Biochem. J.*, **73**, 86 (1959).
(12) Gagen, W., and Holme, J., *Phys. Chem.*, **68**, 723 (1964).
(13) Tanford, C., "Physical Chemistry of Macromolecules," John Wiley & Sons, Inc., New York, N. Y., 1961, p. 627.
(14) Kruyt, H. R., "Colloid Chemistry," vol. 1, Elsevier Publishing Co., Amsterdam, The Netherlands, 1952, Chap. 7.
(15) Swift, D. L., and Friedlander, S. K., *J. Colloid Sci.*, **19**, 621(1964).
(16) Hidy, G. M., *ibid.*, **20**, 123(1965).
(17) Hidy, G. M., and Lilly, D. K., *ibid.*, **20**, 867(1965).

Some Effects of Chloroquine on Oxidative Processes in Rat Heart

By GLORIA A. ARDUESER* and HAROLD C. HEIM

Chloroquine at a concentration of 5.4×10^{-4} *M* enhanced the oxygen consumption of rat ventricle homogenates respiring in the presence of succinate. This effect was not noted with aged homogenates. Total α-keto acids present after incubation of homogenates with succinate was observed to be diminished when chloroquine was present. The oxidation of malate and β-hydroxybutyrate was inhibited by the addition of chloroquine. Chronic poisoning by this drug did not affect the ability of heart homogenates to utilize β-hydroxybutyrate, but the oxidation of malate was impaired. A purified malic dehydrogenase was not inhibited by chloroquine but, at a concentration of 5.4×10^{-4} *M*, the drug markedly inhibited the oxidation of NADH by a fragmented mitochondrial suspension prepared from rat myocardium.

CHLOROQUINE has been shown to have an unexpectedly wide spectrum of therapeutic uses since its introduction into medicine as an antimalarial. The increased utilization of this drug at fairly high dose levels for extended periods has prompted reconsideration of its potential toxicity.

Visual disturbances, headache, bleaching of hair, electrocardiographic changes, and weight loss have been reported during short-term administration of chloroquine to healthy subjects (1). Electrocardiographic changes, consisting of lowered T wave, ST segment depression, and prolongation of QTc interval have occurred when

Received September 6, 1966, from the School of Pharmacy, University of Colorado, Boulder.
Accepted for publication November 14, 1966.
*Present address: School of Pharmacy, Southwestern State College, Weatherford, Okla.